

Hydrogen diffusion and trapping process around MnS precipitates in α Fe examined by tritium autoradiography

Teppei Otsuka*, Tetsuo Tanabe

Interdisciplinary Graduate School of Engineering and Sciences, Kyushu University, Hakozaki 6-10-1, Higashi-ku, Fukuoka 812-8581, Japan

Received 1 October 2006; received in revised form 26 January 2007; accepted 1 February 2007
Available online 6 February 2007

Abstract

Tritium (hydrogen) accumulation and release processes at MnS precipitates and surrounding α Fe matrix area at room temperature (RT) were studied by means of tritium autoradiography (TARG) using a pseudo-binary alloy of Fe–MnS. Hydrogen accumulation at the MnS precipitates at RT was clearly observed but only at a limited occasion. The process involves diffusion, solution and trapping in a complex way including a temperature effect. TARG is proved to be a very good technique to obtain hydrogen area profiles in a near surface region, whereas it is only a snap shot at a particular time and temperature. It could lead us to a totally different interpretation of the accumulation process without detailed dependencies of hydrogen diffusivity and solubility in inclusion species and α Fe on temperatures.

© 2007 Elsevier B.V. All rights reserved.

Keywords: Manganese sulfide; Ferritic steel; Hydrogen; Diffusion; Tritium autoradiography

1. Introduction

Various inclusions and precipitates in steels have been attributed to a cause of hydrogen (H) embrittlement [1–4]. Tritium autoradiography (TARG) developed in 1970s has been applied to demonstrate H accumulation or trapping at them [5–9]. Although many works were devoted to determine binding energies or trapping energies of H, there remain wide discrepancies among data in literatures [10–12]. In addition, unfortunately, most of the data were measured by something like thermal desorption techniques, and extrapolation of the data to lower temperatures could result in large errors.

One of the main reasons for a difficulty to study the H embrittlement is in its low temperature nature. In addition, the amount of H involved in practical embrittlement phenomena is quite tiny and hard to detect. In the present study, we have used pseudo-binary alloys of Fe–MnS to simulate H accumulation at the MnS precipitates in the steels and applied TARG to investigate H trapping at MnS as well as H migration in the α Fe matrix surrounding MnS particles at room temperature (RT).

2. Experimental

A pseudo-binary alloy of Fe–MnS was supplied by the Iron and Steel Institute of Japan. The alloy was manufactured to be used as a standard steel to determine MnS content in steels [13]. The nominal chemical compositions of the alloy were: 0.5% Mn, 0.024% Sn, 0.002% C, 0.002% Si, 0.0069% O and balance Fe. Additionally, 0.023% S was certified to be included in the chemical form of MnS embedded in a α Fe matrix. In the alloy, MnS were precipitated as spheres and/or cylinders elongated along the working direction. Then they were easily distinguished from the matrix as black spheres with 1.5 μ m in an average diameter in a scanning electron microscope (SEM).

Sample disks of 10 mm in diameter and 2 mm in thickness were cut from the alloy, subsequently, their top and bottom surfaces were mechanically polished and mirror finished. Hydrogen (H) and tritium (T) loading was performed by a conventional electrolytic loading cell with the sample disk as a cathode in a 0.1 M NaOH tritiated aqueous solution (specific activity: 1.85 PBq m⁻³, T/H = 1.5 \times 10⁻⁵). Two Pt anode plates were arranged parallel to the cathode sample disk to ensure uniform H and T loading. The loading was made with a sufficiently low current density of 3 A m⁻² at RT for 24 h to avoid an unexpected heating of the sample disk and extremely high condensation of H/T in the sample surfaces. After the loading, the sample surface was ultrasonically cleaned with de-ionized water, which took a little time, 3.0 \times 10² s at maximum. For the H/T loaded samples, two different experiments were carried out; one was the measurement of T evolution from the sample and the other was to make TARG for the sample surface.

The T evolution represented a total amount of released T from a sample. Just after the H/T loading, the sample (sample O) was immersed in a liquid scintillation solution (PCS, GE Healthcare) and time sequences of T accumulation (referred as a T evolution curve) in the solution was measured until

* Corresponding author. Tel.: +81 92 642 4139; fax: +81 92 642 3796.
E-mail address: t-otsuka@nucl.kyushu-u.ac.jp (T. Otsuka).

saturation. From the T evolution curve, an apparent diffusion coefficient was determined.

TARG was made for the surfaces of following three samples; one was taken at 3.6×10^3 s, which was a minimum requirement for preparation of TARG as depicted below, just after the loading (referred as sample I), the other two were kept at RT in the atmosphere for 2.5×10^4 and 8.6×10^4 s after the loading (respectively, referred as samples II and III).

An H/T loaded sample surface was coated by a photographic film made of a 20 nm collodion film and a monolayer of nuclear photographic emulsion of AgBr (Kodak EM-1). The former, which avoids any chemical reactions of AgBr in the emulsion film with the sample, was made with the dipping method and the latter with the wire-loop method in a photo darkroom. The photographic film was automatically exposed to tritium β electrons with averaged energy of 5.7 keV from the sample. To get clear TARG in the present T loading condition, long exposure time (1.7×10^6 s) was required. Hence the exposure was done at liquid nitrogen (liq. N₂) temperature to avoid H/T migration and release. After the exposure at liq. N₂ temperature, development and fixation were carried out without peeling the photographic film from the sample surface. The average size of the AgBr particles in the nuclear emulsion was 0.2 μm and consequently the size of the Ag particles after the development of the photographic film was 0.2–0.5 μm .

TARG, i.e. distribution of the Ag particles on the surface of the Fe–MnS pseudo-binary alloy, was observed with SEM. The obtained autoradiographs were processed and analyzed with using a public domain ImageJ program developed at the U.S. National Institutes of Health [14].

3. Results

3.1. Evolution experiment

Fig. 1 shows a time sequence of amount of released T from the sample O into a liquid scintillation solution at RT. After the saturation of the released T at RT, the temperature of the solution together with the sample was raised to 323 K and no additional T release was observed. This indicated that most of T except those trapped with a very high trapping energy (if any) was released. According to the simple approximation of isotopic effects on the electrolysis of tritiated water, dissolution and evolution of H and T in metals [15], we assumed here that the T/H ratio in the sample was almost same as that of the tritiated water (1.5×10^{-5}) used for the loading. As a result, the amount of evolving H was estimated to be 1.5×10^{-6} atom H/atom Fe.

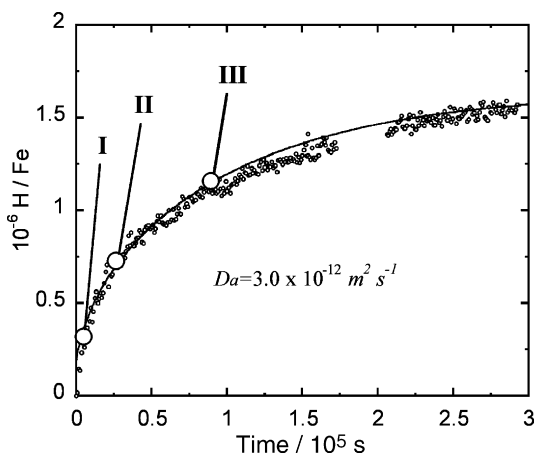


Fig. 1. The time sequence of amount of released H at RT.

Suppose uniform H distribution being attained by the loading, an analytical solution for H release from the sample is given as

$$\frac{M_t}{M_\infty} = 1 - \frac{32}{\pi^2} \sum_{n=0}^{\infty} \frac{1}{(2n+1)^2} \exp \frac{-(2n+1)^2 \pi^2 D_a t}{a^2} \\ \times \sum_{n=1}^{\infty} \frac{1}{\beta_n^2} \exp \frac{-4\beta_n^2 D_a t}{b^2}$$

according to the Fick's diffusion equation for the geometry of the sample disk, where M_t is the amount of released H at a time t ; M_∞ , the total H loaded; D_a , an apparent diffusivity of H; β_n , roots of zero order Bessel function; a and b , are the thickness and diameter of the disk, respectively. The solid line is a calculated result for D_a being $3.0 \times 10^{-12} \text{ m}^2 \text{ s}^{-1}$, which is 3 orders of magnitude smaller than that for pure Fe ($9.1 \times 10^{-9} \text{ m}^2 \text{ s}^{-1}$) [16].

3.2. Tritium autoradiography around MnS

TARG of samples I–III are shown in Fig. 2(a–c), respectively. Those are snap shots of surface tritium distribution during the evolution at respective times indicated in Fig. 1. In TARG, small white dots corresponding to Ag particles were clearly distinguished from a black MnS sphere embedded in a dark grey αFe background. Since Ag contrast, i.e. an area density of Ag particles, directly reflected to the abundance of T(H), hereafter, it is presumed that an area density of Ag particles is proportional to H concentration in a volume within 0.3 μm from the surface, which is an escaping depth of 5.7 keV β electrons of T in αFe .

As seen in Fig. 2(a), for the sample I kept only 3.6×10^2 s after the loading, H atoms uniformly distributed over the αFe matrix except for the area surrounding MnS where the H concentration was a little depleted. More careful inspection of TARG clearly shows radial concentration gradient in the MnS surrounding area as indicated in Figs. 3(a) and 4(a). The former is one of magnified TARG for the sample I together with its computer processed black and white image (Fig. 3(b)). For 10 MnS precipitates in the sample, area densities of the Ag particles were determined and plotted against a radial distance from the interface of Fe–MnS to the radial direction in the area surrounding MnS as shown in Fig. 4(a).

In the specimen II, the H concentration in the matrix decreased as expected. However, H concentration in the MnS surrounding area increased as shown in Fig. 2(b). It is noted that the digitized image for the sample II clearly shows H concentration gradients, but was opposite to the sample I, as shown in Fig. 4(b). After longer release time (see Fig. 2(c)), the H concentration decreased, showing rather uniform except for special areas as seen as a line corresponding to a scratch originating from mechanical polishing and the boundary between the matrix and the MnS precipitate (Fe–MnS interface). This result corresponded well to the fact that H atoms were rather strongly trapped in the defects at the scratch and the Fe–MnS interface than in the αFe interstitials.

All those results clearly show H trapping by MnS as already demonstrated in [5–9]. Nevertheless, the trapping process is not simple to understand and is discussed in the following.

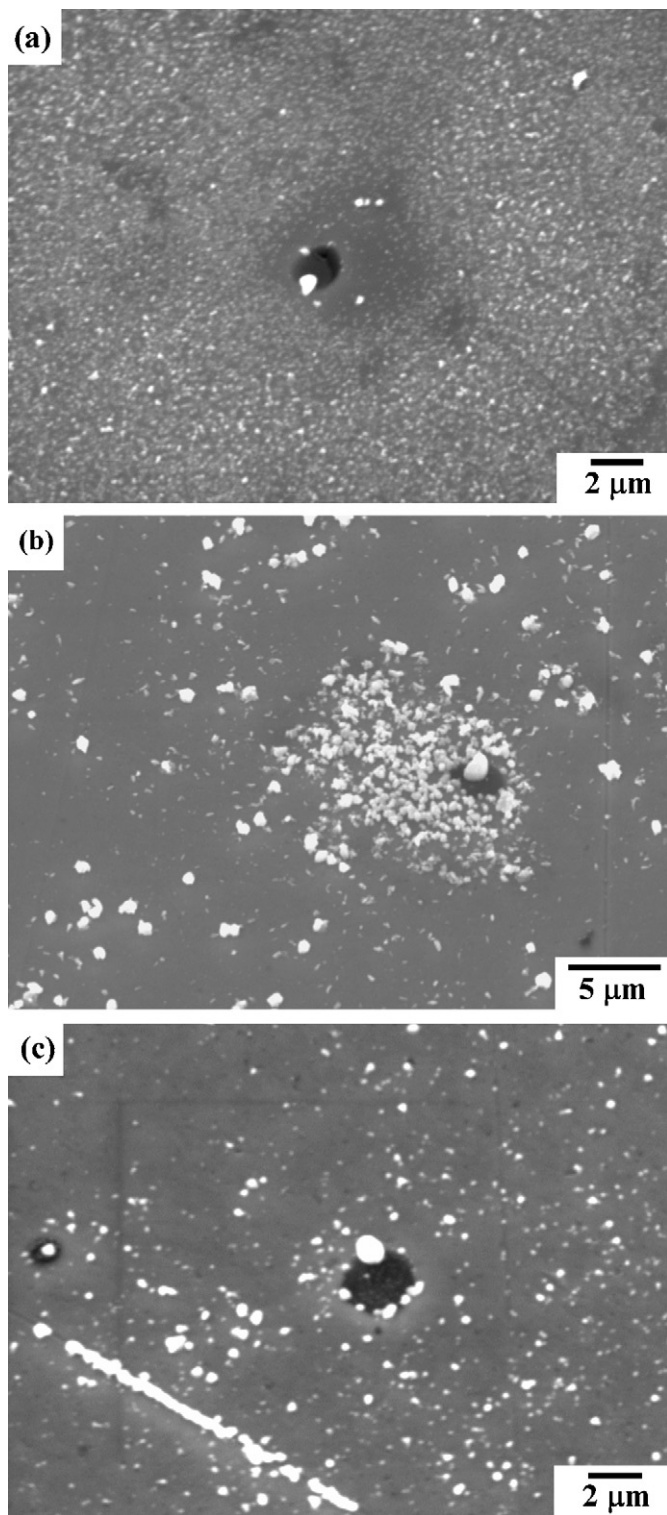


Fig. 2. TARG for samples I, II and III kept at RT (a) 3.6×10^2 s, (b) 2.5×10^5 s and (c) 8.6×10^5 s, respectively, after loading.

4. Discussion

We first discuss H migration in the α Fe matrix, particularly the MnS surrounding area. As indicated in Fig. 2(a and b), H atoms were clearly depleted in the MnS surrounding area for the sample I, while the opposite for the sample II. Supposing

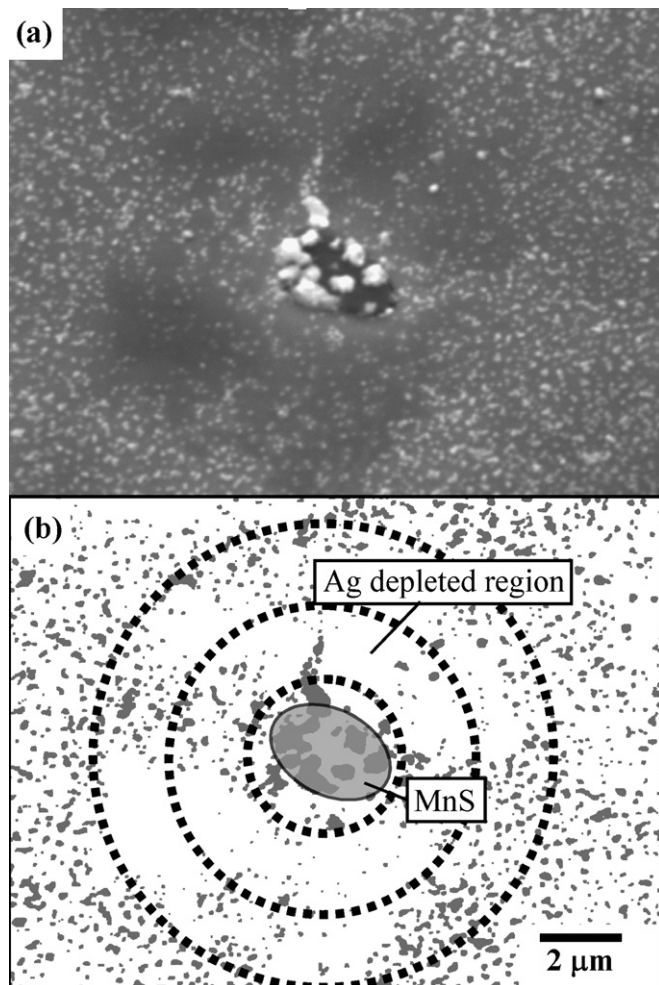


Fig. 3. (a) Magnified TARG for sample I and (b) computer processed binary image in the same area.

H diffusion in the matrix was homogeneous, i.e. the diffusivity is independent on locations, then the H depletion should be attributed to the H diffusion to the Fe–MnS interface. Since the Fe–MnS interface is incoherent owing to the larger thermal expansion coefficient of MnS ($18.1 \times 10^{-6} \text{ K}^{-1}$) than α Fe ($12.5 \times 10^{-6} \text{ K}^{-1}$), there should be some gap at the interface. Hence H in the matrix could be released at this interface gap in addition to the sample surfaces. For the case appeared in Fig. 3(a), the concentration profile in the MnS surrounding area can be modeled by a Fick's diffusion equation for a 2D cylindrical geometry numerically calculated by a finite difference method. With a curve fitting method, an apparent diffusion coefficient for the sample I (diffusion from the matrix to the Fe–MnS interface gap) was determined to be in the order of $10^{-15} \text{ m}^2 \text{ s}^{-1}$, which is much smaller than the apparent diffusion coefficient, $D_a = 3.0 \times 10^{-12} \text{ m}^2 \text{ s}^{-1}$, determined for overall H release from the sample O in Fig. 1. Thus, the concentration gradient in the MnS surrounding area could not be attributed to a simple H release from the matrix to the gap. This suggests that some H atoms must be supplied from MnS. Actually, the gradient was opposite for the sample II (see Fig. 4(b)) supporting the H supply from MnS.

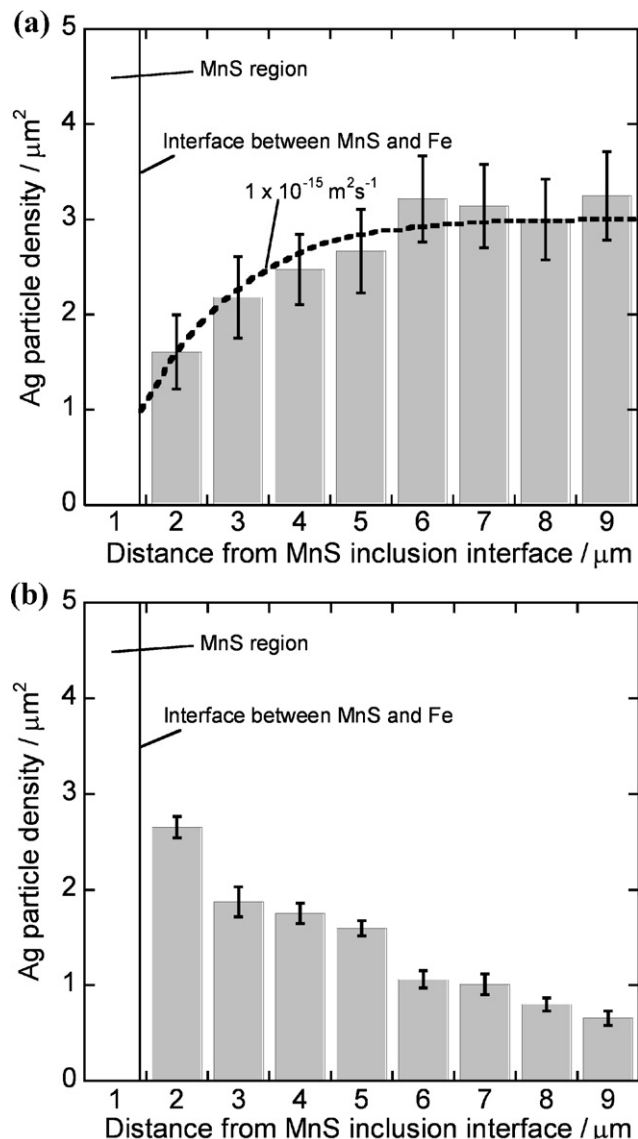


Fig. 4. H profile along the radial direction in the MnS surrounding area for samples I and II (a) 3.6×10^2 s and (b) 2.5×10^5 s after loading.

Our tentative explanation for the present observation is the following: initially, because of long time loading under a high H fugacity, the H concentration must be saturated to give homogeneous concentration throughout the sample. Immediately after stopping the loading, H release begins. In order to give the H profile shown in Fig. 3(a), the initial H concentration of the matrix would be higher than that of MnS and/or H release from the matrix is faster than that from MnS. After a certain time, owing to faster diffusion in the matrix, their H concentration is significantly reduced, while the slower diffusion in MnS does not allow H release, resulting in a higher concentration in MnS. Consequently, H supply from MnS modifies the concentration profile in the matrix; firstly it delays the H release from the Fe–MnS interface and afterwards overwhelms the release from the matrix.

It was found that the H concentration in the MnS surrounding area increased from the samples I to II. According to the sim-

ple diffusion release model with the assumption of the initially homogeneous concentration, it must decrease with time. Consequently, the higher concentration around MnS at a longer time after the loading lead us to an idea that the MnS surface should trap H atoms and significant reduction of H solubility in MnS occurs with lowering fugacity and decreasing temperature, i.e. H dissolved in MnS during the loading remains longer time and easily precipitates as something like hydride or accumulates in trapping sites including its surface. Thus, to attain such situation around MnS, the H diffusivity must be larger in the αFe matrix than that in MnS and the activation energy for H solution (the heat of solution, ΔH_s) might be opposite relationship between them.

Since, as indicated in Fig. 1, the apparent diffusivity that was $3.0 \times 10^{-12} \text{ m}^2 \text{ s}^{-1}$ at RT for overall H release is still much slower than that for pure Fe, the matrix itself should trap large amount of H to increase the apparent solubility. However, the MnS precipitates clearly influence the H release from the matrix surrounding them. This means that significant amount of H initially dissolved in MnS should be released to influence its surrounding matrix. To ensure large amount of H release from MnS, ΔH_s in MnS might be fairly large. Eventually, the storage at liq. N_2 temperature to obtain TARG could enhance the H release from the MnS to the αFe matrix to be trapped.

Because no data for the H solubility and trapping in MnS have been available, all above discussion is speculative and needs to be confirmed by additional experiments at different temperatures. Nevertheless, the present work demonstrates that the simple H profiling, not only TARG, but also depth profiling using nuclear analysis and SIMS is only a snap shot and could give totally different conclusions on H accumulation at the inclusion species in αFe without detailed dependences on time and temperature.

5. Conclusions

In order to examine H diffusion and trapping process around MnS in αFe , TARG was applied to the Fe–MnS pseudo-binary alloy at different evolution time after H(T) loading. TARG clearly shows hydrogen trapping in MnS. However, the accumulation or release process are found to involve diffusion, solution and trapping in a complex way.

Assuming that αFe has higher hydrogen diffusivity than MnS, while MnS has higher heat of solution than αFe , the present observation is interpreted as follows.

Initially, H(T) was loaded homogeneously in the matrix except in the MnS precipitates and surrounding area, where the H concentration depleted a little. Because of large H diffusivity in the matrix, their H concentration was significantly decreased with time. On the other hand, owing to the slower diffusion and larger trapping energy in MnS, H remained longer in MnS. Consequently, the H concentration became higher in MnS. Furthermore, some H in the MnS seems to be released into the matrix.

Although the interpretation is speculative, the present work demonstrates that the simple H profiling, not only TARG, but also depth profiling using nuclear analysis and SIMS is only a snap shot and could give totally different conclusions on H accu-

mulation at the inclusions in α Fe without detailed dependences on time and temperature.

References

- [1] R.P. Frohberg, W.J. Barnett, A.R. Troiano, *Trans. ASM* 47 (1954) 892–925.
- [2] G.M. Pressouyre, I.M. Bernstein, *Acta Metall.* 27 (1978) 89–100.
- [3] K. Takai, Y. Homma, K. Izutsu, et al., *J. Jpn. Inst. Met.* 60 (1996) 1155–1162.
- [4] Y. Murakami, N.N. Yokoyama, J. Nagata, *Fatigue Fract. Eng. Mater. Struct.* 25 (2002) 737–746.
- [5] C.P.D. Oliveira, M. Aucouturier, P. Lacombe, *Corrosion* 36 (1980) 53–59.
- [6] D.L. Tuyen, B.E. Wilde, *Corrosion* 39 (1983) 258–265.
- [7] M. Garet, A.M. Brass, C. Haut, et al., *Corros. Sci.* 40 (1998) 1073–1086.
- [8] T. Otsuka, H. Hanada, H. Nakashima, et al., *Fusion Sci. Technol.* 48 (2005) 708–711.
- [9] H. Hanada, T. Otsuka, H. Nakashima, et al., *Scripta Mater.* 53 (2005) 1279–1284.
- [10] H.G. Lee, J.-Y. Lee, *Acta Metall.* 32 (1983) 131–136.
- [11] W.C. Luu, J.K. Wu, *Mater. Lett.* 24 (1995) 175–179.
- [12] E. Serra, G. Benamati, O.V. Ogorodnikova, *J. Nucl. Mater.* 255 (1998) 105–115.
- [13] K. Narita, *Tetsu-to-Hagane* 1 (1986) 24–31.
- [14] W.S. Rasband, ImageJ, Bethesda, U.S. National Institutes of Health, 1997–2005, <http://rsb.info.nih.gov/ij/>.
- [15] J.P. Laurent, G. Lapasset, *Int. J. Appl. Radiat. Isot.* 24 (1973) 213–230.
- [16] T. Tanabe, Y. Yamanishi, S. Imoto, *J. Jpn. Inst. Met.* 25 (1984) 1–10.